Assessment of Ecological Vulnerability on Northern Sand Prevention Belt of China Based on the Ecological Pressure–Sensibility–Resilience Model

Xiufen Li [1], Lining Song [2,3,4,*], Zunbo Xie [1], Tian Gao [2,3,4], Tingting Wang [1], Xiao Zheng [2,3,4], Jiang Liu [1] and Limin Liu [1]

1   Agronomy College, Shenyang Agricultural University, Shenyang 110866, China; lixiufen2019@syau.edu.cn (X.L.); hotm997020517@hotmail.com (Z.X.); wtt1204@hotmail.com (T.W.); liujiang@syau.edu.cn (J.L.); liulimin1968@syau.edu.cn (L.L.)
2   CAS Key Laboratory of Forest Ecology and Management, Institute of Applied Ecology, Chinese Academy of Sciences, Shenyang 110016, China; tiangao@iae.ac.cn (T.G.); xiaozheng@iae.ac.cn (X.Z.)
3   Qingyuan Forest CERN, Chinese Academy of Sciences, Shenyang 110016, China
4   Liaoning Key Laboratory for Management of Non-Commercial Forests, Shenyang 110016, China
*   Correspondence: liningsong@iae.ac.cn; Tel.: +86-24-83970473; Fax: +86-24-83970300

Abstract: Quantitative assessment of ecological vulnerability is of great significance for ecological protection and restoration in ecologically vulnerable regions. Here, the ecological vulnerability of the northern sand prevention belt (NSPB) of China was assessed using an ecological pressure–sensibility–resilience model from 2000 to 2015. Results showed that the ecological vulnerability index (EVI) displayed low values in the eastern part and high values in the western part of the study region. The EVI ranged from 0.29 to 1.32 in 2000, with the mean value of 0.88, whereas it averaged 0.78 in 2015, ranging from 0.21 to 1.26. Decreasing EVI from 2000 to 2015 indicated that the ecological status has been improved. Moreover, the area proportion of moderately, heavily, and extremely ecological vulnerability levels occupied approximately 87% in both 2000 and 2015, indicating a high ecological vulnerability level. Furthermore, the change in area proportion of different ecological vulnerability levels were associated with the change in the spatial distribution of vegetation coverage, indicating that eco-environmental protection projects were indeed effective. These findings indicated that differential strategies in different restoration zones should be adopted, especially in the western parts of the study region, and eco-environmental protection projects should be reinforced to improve the ecological restoration.

Keywords: ecologically vulnerable regions; ecological protection and restoration; principal component analysis; ecological restoration projects

1. Introduction

Since the middle of the 20th century, the global ecological environment has been altered dramatically accompanying the increase of human activities and global climate change [1]. Ecosystem degradation such as deforestation, soil degradation, desertification, and loss of biodiversity has become one of the most prominent environmental problems around the world, especially in ecologically vulnerable regions [2,3], which would threaten ecosystem services and human well-being [4]. Ecological vulnerability is a specific attribute of ecosystems, which indicates the resistance and resilience of an ecosystem to external interference within a certain region [4–9]. It is an important evaluation indicator reflecting regional ecological status and the degree of ecosystem stability, which also is the key content in global change and sustainable development [3,10]. Therefore, a quantitative assessment of the vulnerability of ecosystems is the scientific basis of adapting and mitigating climate changes and is of great significance for ecological protection and restoration and ecological environment management [1,3,11,12].

To assess the ecological vulnerability of ecosystem, a series of quantitative assessment models have been developed based on the different principles and purposes of assessment, mainly including the pressure–sensibility–resilience model [3,4,13], exposure–sensitivity adaptation model [14,15], resilience–exposure–sensitivity model [16], pressure–state–response model [4,17], society–ecology model [18], influencing performance–stress factors model [19], natural causes–results model [20], etc. In these quantitative assessment models, the weights of the evaluation indices are generally determined using principal component analysis [8,21,22], fuzzy methods [23], analytic hierarchy processes [24,25], artificial neural network methods [26], etc. Although several quantitative models, combined with methods for determining the weights of the evaluation indices, have been developed to assess the ecological vulnerability, there is no uniform standard for the selection of the evaluation indices in different regions and research scales [4,27]. Therefore, it is necessary to explore the ecological vulnerability assessment further. Moreover, most of the current studies focused on the ecological vulnerability of wetlands [23,28,29], river basins [12,16,17,30], coastal zones [24,31,32], administrative units such as cities [4,33,34], and forest ecosystems [35], while little knowledge exists about the ecological vulnerability of sandy land ecosystems in semiarid and arid regions [7,24].

The northern sand prevention belt (NSPB) is a significant component of the "Two Ecological Shelters and Three Belts" national ecological security shelter framework in China, which is to improve the environment and maintain national ecological security (the state of the environment and ecosystem in a nation) [36]. During the past few decades, the irrational use of resources has led to a series of ecological problems such as forest and grass degradation, land desertification, and serious soil erosion in the northern sand prevention belt [1,37]. Ecological restoration is widely implemented as a means of restoring ecosystem functions, reducing ecological vulnerability, and promoting harmony between humans and land [38]. Therefore, large-scale ecological restoration projects in the NSPB such as the Three-North Afforestation Program (TNAP), Sand Prevention and Control Projects, and Grain for Green Program (GGP) have been implemented to improve the local ecological environment [3,39]. Although several studies have shown that the ecological environment in the northern sand prevention belt has been improved accompanying by the implementation of ecological restoration projects [1,37,40], the ecological vulnerability of NSPB is still fully unknown, which is a disadvantage of ecological protection and restoration in this region.

In this study, we used the ecological pressure–sensibility–resilience model, combined with principal component analysis, to assess the ecological vulnerability in the NSPB from 2000 to 2015. This was because the pressure–sensibility–resilience model has the advantages of the comprehensive evaluation of ecological vulnerability, data availability, and strong regional pertinence, which has been successfully widely utilized in studies on ecologically fragile areas over the years [41]. In addition, this model is constructed based on the connotation of ecosystem stability and has a clear causal relationship, which covers three major components of ecological vulnerability, namely, ecological sensitivity, ecological resilience, and ecological pressure [3]. Furthermore, principal component analysis (PCA) can provide information about the most meaningful parameters, which are those that describe the whole data set and allow for data reduction with minimal loss of the original information [42]. The specific objectives of this study were to quantify the spatial-temporal variations of the ecological vulnerability of the northern sand prevention belt in northern China. The results of this study would provide a scientific reference for decision makers to make better ecological protection policies.

2. Materials and Methods

2.1. Study Region

This study was conducted in the northern sand prevention belt of China (71°34′ E–125°43′ E, 26°45′ N–43°53′ N) (Figure 1). The northern sand prevention belt includes three parts: the Tarim sand-prevention belt, the Hexi Corridor sand-prevention belt, and

the Inner Mongolia sand-prevention belt, whose main functions are being windproof and providing sand fixation and grassland protection (Figure 1) [36]. The total area of the northern sand prevention belt is 8.69×10^5 km^2. This region has a semiarid and arid climate. The mean annual precipitation ranges from 30 to 450 mm, with 80–90% of precipitation occurring between May and September. The mean annual temperature ranges from 1.9 to 13.5 °C [37]. The main soil types in the study region are aeolian sandy soil, brown desert soil, and brown soil. The wind speed is relatively large, with an average speed of blowing sand of 7.3 m s^{-1} (more than 5 m s^{-1}). The vegetation coverage is low, exhibiting relatively high in the eastern part of the study region and low in the western part of the study region. This region is the typical agropasture ecotone, and the vegetation types are composed of desert landscape, grassland landscape, and forest landscape, with 67% of the desert landscape and grassland landscape [37].
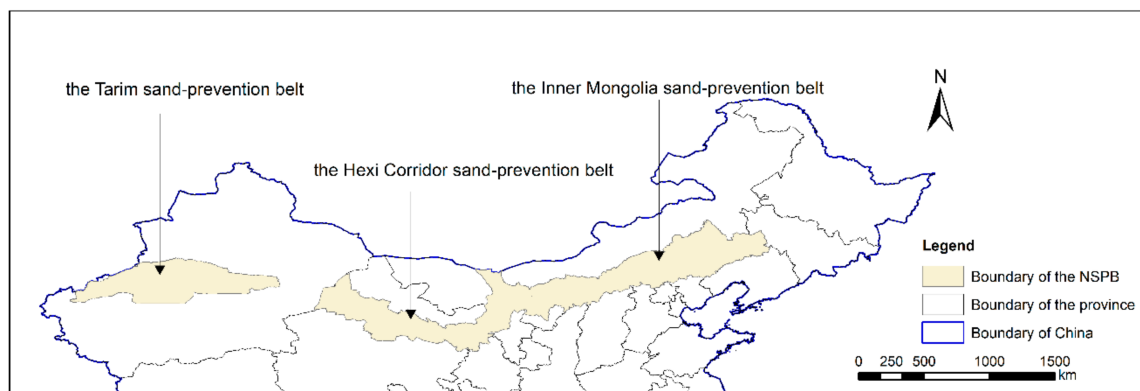

Figure 1. The location of the study area. NSPB: the northern sand prevention belt.

2.2. Data Sources

The data used in the present study mainly included remote sensing, meteorological, socioeconomic, and basic vector data. Meteorological datasets were obtained from the national meteorological science data sharing service platform (http://data.cma.cn/, accessed on 7 April 2020), which included the monthly mean temperature data and monthly rainfall in 2000 and 2015. Digital elevation model (DEM) data were derived from the sharing platform of Geospatial Data Cloud (http://www.gscloud.cn/, accessed on 5 August 2020) with a spatial resolution of 30 m. DEM data were used to produce index layers of the slope. Moreover, land use/cover (LULC) data in 2000 and 2015 was provided by the Data Center for Resources and Environmental Sciences, Chinese Academy of Sciences (optimization of ecosystem services pattern in two ecological barriers and three shelters of National Key Research and Development Programs in China). The population density data used were derived from the WordPop (https://www.worldpop.org/, accessed on 24 November 2020), with a spatial resolution of 100 m in 2000 and 2015, and each grid pixel represents the number of people per hectare. Gross domestic product (GDP) data and soil type data were derived from the Data Center for Resources and Environmental Sciences, Chinese Academy of Sciences. The GDP data were obtained from the China GDP spatial distribution grid datasets with a spatial resolution of 1000 m in 2000 and 2015, and the soil type data were used to calculate the soil erodibility factor with a spatial resolution of 1000 m. The normalized difference vegetation index (NDVI) data were also obtained from the Data Center for Resources and Environmental Sciences, Chinese Academy of Sciences (http://www.resdc.cn/, accessed on 23 October 2019). In the present study, the net primary productivity (NPP) in 2000 and 2015 were estimated based on the Carnegie–Ames–Stanford Approach (CASA) model using a moderate resolution imaging spectroradiometer (MODIS) and meteorological datasets.

2.3. Assessment Index System of Ecological Vulnerability

Based on existing evaluations of the ecological vulnerability, the northern sand prevention belt is considered to exhibit typical "pressure–sensitivity–resilience" (PSR) characteristics [34,43,44]. Therefore, the assessment index system of ecological vulnerability for the study region was established based on the three PSR dimensions. In the PSR model, a total of 13 indicators (Table 1) were selected from the 3 levels of ecological sensitivity, ecological resilience, and ecological pressure, following the principles of scientificity, dominance, feasibility, qualitative and quantitative and combining with the performance and main causes of ecological vulnerability in the NSPB. In addition, these indicators were selected also by referring to the relevant study and characteristics of the geographical area. These indicators were introduced for evaluating the ecological security of the sand prevention belt of northern China due to their widespread availability and adaptability [27,34]. Ecological pressure refers to the degree of disturbance from the external environment that ecosystems usually from human activity and economic pressure [45], e.g., population density (people·km^{-2}) and gross domestic product per capita (GDP, RMB) in the present study. Ecological sensitivity refers to the degree of response of the ecosystem after pressure, which is determined by the system's environmental factors [34,46]. Therefore, eight ecological environmental factors, namely, elevation (m), slope (°), soil erodibility factor, land use types, precipitation (mm), temperature (°C), humidity index, and windy days (day), were selected to evaluate the ecological sensitivity of the study region. Ecological resilience refers to the capacity of a system to resist disturbance and reorganize while changing to retain essentially the same functions, structures, identities, and feedbacks [47], expressed in terms of net primary productivity (g C·m^{-2}·a^{-1}), vegetation coverage, and amount of sand fixation (t·hm^{-2}) in the present study.

Table 1. Assessment index of the ecological vulnerability using the pressure–sensibility–resilience model for northern sand prevention belt of China.

Criterion Layer	Feature Layer	Indicator Layer	Attributes
Pressure	Human activity Pressure	Population density	Positive
	Economic pressure	GDP per capita	Positive
Sensibility	Terrain	Elevation	Positive
		Slope	Positive
	Earth's surface	Soil erodibility factor *	Positive
		Land use types	Positive
	Meteorology	Precipitation	Negative
		Temperature	Negative
		Humidity index	Negative
		Windy days	Positive
Resilience		Net primary productivity	Negative
		Vegetation coverage	Negative
		Amount of sand fixation	Negative

Note: * Soil erodibility factor (EF) is calculated by equation [48]: EF = [29.9 + 0.31Sa + 0.17Si +0.33 (Sa/Cl) − 0.29OM − 0.95CaCO$_3$]/100, where Sa is sand content (%), Si is silt content (%), Sa/Cl is the ratio of sand to clay, SOM is soil organic matter content (%), and CaCO3 content (%).

2.4. The Index of Ecological Vulnerability

After preprocessing of each index, the index was standardized using the following Equations (1) and (2) [21,34]:

$$\text{Positive indicator}: \; X'_{ij} = \frac{X_{ij} - X_{j-\min}}{X_{j-\max} - X_{j-\min}} \tag{1}$$

$$\text{Negative indicator}: \; X'_{ij} = \frac{X_{j-\max} - X_{ij}}{X_{j-\max} - X_{j-\min}} \tag{2}$$

where X'_{ij} represents the normalized value of index j in grid cell i, X_{ij} represents the actual value of index j in grid cell i, and $X_{j\text{-}min}$ and $X_{j\text{-}max}$ are the minimum and maximum values of index j in the study region, respectively.

After data standardization, the principal component analysis (PCA) was employed to develop a model used to evaluate ecological vulnerability based on 13 selected parameters from within 3 groupings for the study region [49]. The PCA contributed to simplifying the data, reducing the number of original data types, and retaining the original data to the greatest extent [3]. The PCA was used to compress all 13 indicators (Table 1) and transform the indicators data into 13 representatives comprehensive principal components (Table 2). The ranking of the principal components in order of their significance is denoted by the eigenvalues associated with the vector for each principal component, and the proportion of the total variance explained by each principal component was calculated. If the accumulated contribution (proportion) represents over 85% of the total variance, the remaining components can be ignored (Table 2) [45,49]. The final evaluation value was obtained using the following formula [3]:

$$EVI = r_1PC_1 + r_2PC_2 + \cdots + r_qPC_q \tag{3}$$

where EVI represents the ecological vulnerability index, r_q is the contribution ratio of the principal component PC_q, PC is the principal component, and q is the number of principal components retained. According to the natural breakpoint method, the EVI can be divided into five levels: slightly (0–0.4), lightly (0.4–0.6), moderately (0.6–0.8), heavily (0.8–1.0), and extremely (>1.0) vulnerability [34].

Table 2. Eigenvalues, contribution rates, and cumulative contribution rates for the index of the ecological vulnerability.

Principal Component	2000			2015		
	Eigenvalue	Contribution	Cumulative Contribution	Eigenvalue	Contribution	Cumulative Contribution
1	4.657×10^{-2}	50.066	50.066	4.934×10^{-2}	49.265	49.265
2	1.671×10^{-2}	17.968	68.034	1.725×10^{-2}	17.225	66.490
3	1.308×10^{-2}	14.058	82.092	1.133×10^{-2}	11.317	77.807
4	6.112×10^{-3}	6.571	88.663	9.997×10^{-3}	9.981	87.788
5	3.537×10^{-3}	3.803	92.466	4.434×10^{-3}	4.427	92.214
6	2.417×10^{-3}	2.598	95.064	2.076×10^{-3}	2.072	94.287
7	2.037×10^{-3}	2.190	97.253	1.943×10^{-3}	1.940	96.227
8	1.076×10^{-3}	1.157	98.410	1.641×10^{-3}	1.638	97.865
9	8.602×10^{-4}	0.925	99.334	1.052×10^{-3}	1.050	98.915
10	6.047×10^{-4}	0.650	99.985	6.841×10^{-4}	0.683	99.598
11	1.876×10^{-5}	0.010	99.994	3.560×10^{-4}	0.356	99.953
12	1.949×10^{-5}	0.006	99.999	4.491×10^{-5}	0.045	99.998
13	3.235×10^{-7}	0.0001	100	1.890×10^{-6}	0.002	100

Note: The eigenvalue represents the total amount of variance that can be explained by a given principal component, while the contribution is the proportion of the total variance explained by each principal component. In addition, cumulative contributions are the cumulative proportion of the total variance explained by the principal component.

3. Results

3.1. Spatiotemporal Dynamics of the Indicators

The gross domestic product per capita (GDP) ranged from 0 to 115,382 RMB in 2000 and from 0 to 179,735 RMB in 2015 (Figure 2a,b). However, it displayed a low value in 2000, and area proportion of less than 15,000 RMB (1906 EUR, calculated based on the average exchange rate in 2020) occupied 99% (Figure 2a), whereas area proportion of more than 15,000 RMB for GDP accounted for over 92% in 2015 (Figure 2b). Moreover, the density of the population varied between 0 and 5879 people per square kilometer and between 0 and 11,991 people per square kilometer in 2000 and 2015, respectively. However, the area proportion of the population density less than 25 people per square kilometer accounted for

88% in 2000, whereas the area proportion for the population density less than 100 people per square kilometer occupied 94% in 2015 (Figure 2c,d).
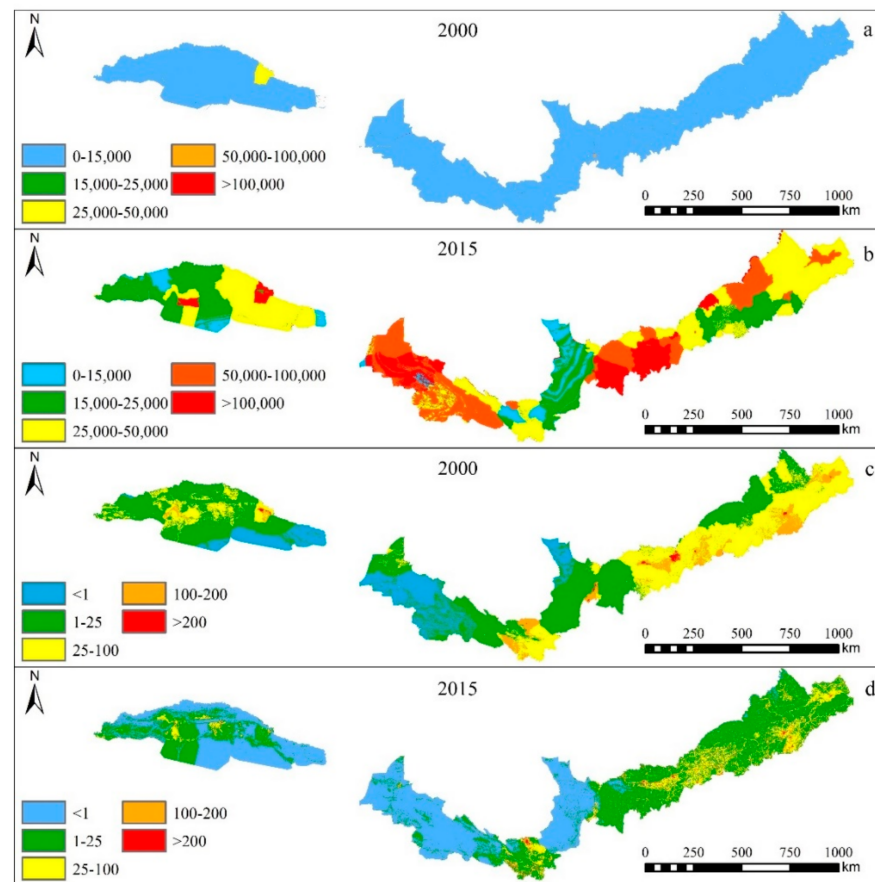

Figure 2. Spatial distribution of gross domestic product per capita (GDP, (**a**,**b**)) and population density (**c**,**d**) in the northern sand prevention belt of China in 2000 and 2015.

The elevation displayed the higher values in the western part of the study region and lower values in the eastern part of the study region (Figure 3a). The elevation of the study region ranged from 0 to 6932 m, and approximately 53.9% of the total area was located in 750–1500 m. Moreover, the slope of the study region was mainly ≤6° (ranging from 0 to 40°), whereas the slope of the study region more than 6 ° is mainly located in the Tianshan Mountain, Qilian Mountain, and Yinshan Mountain (Figure 3b). Furthermore, the soil erodibility factor in the study region ranged from 0 to 0.93, and it was within 0.6–0.7 for more than 61.8% of the total area (Figure 3c). Moreover, grassland was the main land-use type in the study region, accounting for 37.81% and 37.56% of the total area of the study region in 2000 and 2015, respectively (Figure 3d,e). From 2000 to 2015, the area of shrubland and grassland decreased by 4646 and 2324 km^2, respectively, whereas the area of cropland and built-up lands increased by 3467 and 3607 km^2, respectively.
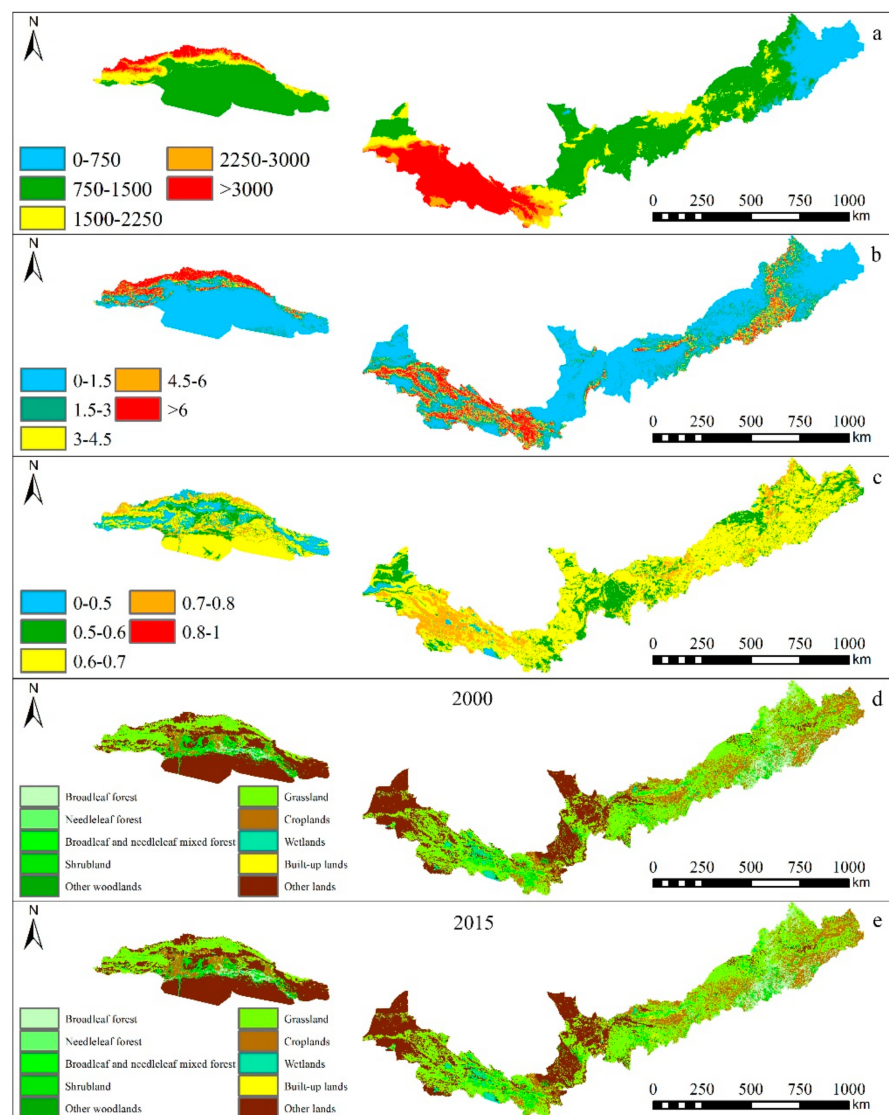
Figure 3. Spatial distribution of elevation (**a**), slope (**b**), soil erodibility factor (**c**), and land use types (2000 and 2015, (**d**,**e**)) in northern sand prevention belt of China.

In the study region, the precipitation ranged from 0.2 to 1006 mm and 0.6 to 1199 mm in 2000 and 2015, respectively, and the region with annual precipitation less than 400 mm accounted for 71% and 74% of the total area in the study region in 2000 and 2015, respectively (Figure 4a,b). However, the annual mean air temperature varied between −0.8 to 13.2 °C in 2000 and between 0.6 to 14.3 °C in 2015 (Figure 4c,d). The region with annual mean air temperature less than 9 °C occupied 76% and 71% of the total area of the study region in 2000 and 2015, respectively (Figure 4c,d). Additionally, the humidity index ranged from 0.11 to 0.93 and from 0.13 to 0.92 in 2000 and 2015 in the study region, respectively, with more than 70% of the total area less than 0.3 in both years (Figure 4e,f). From 2000 to 2015, the windy days in different day classifications decreased (except for the windy days of 10 day), and the region with the windy days of 10 day accounted for 64% of the total area in 2015 (Figure 4g,h).
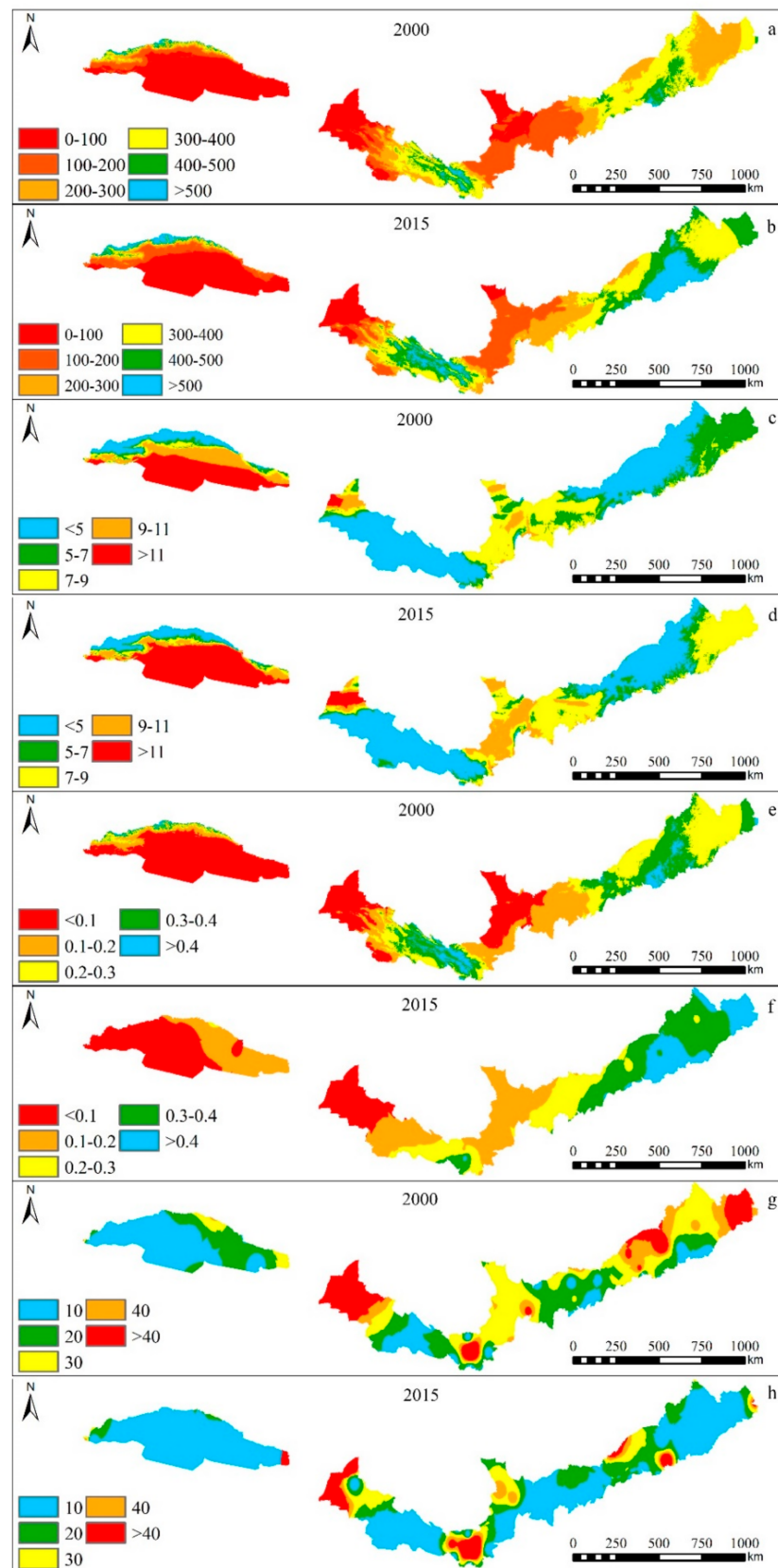
Figure 4. Spatial distribution of annual precipitation (**a**,**b**), annual mean air temperature (**c**,**d**), humidity (**e**,**f**), and the number of windy days (**g**,**h**) in the northern sand prevention belt of China in 2000 and 2015.

The vegetation coverage ranged from 0 to 1 in both 2000 and 2015. However, the vegetation coverage is low in the study region, and more than 66% of the study area had vegetation coverage of less than 0.5 in both 2000 and 2015 (Figure 5a,b). Moreover, the high vegetation coverage was located in the eastern part of the Inner Mongolia sand-prevention belt and the Hexi Corridor sand-prevention belt. Furthermore, the mean vegetation coverage was 0.41 in 2000, whereas it was 0.47 in 2015. In addition, the net primary productivity varied between 0 and 1123.7 g $C \cdot m^{-2} \cdot a^{-1}$ and between 0 and 1307.7 g $C \cdot m^{-2} \cdot a^{-1}$ in 2000 and 2015, respectively. Nevertheless, the net primary productivity was also low, with over 60% of the total area having the net primary productivity less than 50 g $C \cdot m^{-2} \cdot a^{-1}$ (Figure 5c,d). Furthermore, the amount of sand fixation varied between 0 and 38.3 $t \cdot hm^{-2}$ and between 0 and 43.2 $t \cdot hm^{-2}$ in 2000 and 2015, respectively. The amount of sand fixation overall was low, and the region with the amount of sand fixation less than 5 $t \cdot hm^{-2}$ occupied more than 77% of the total study area. From 2000 to 2015, the area with the amount of sand fixation >20 and 5–10 $t \cdot hm^{-2}$ decreased, whereas <5, 15–20 and 10–15 $t \cdot hm^{-2}$ increased (Figure 5e,f).
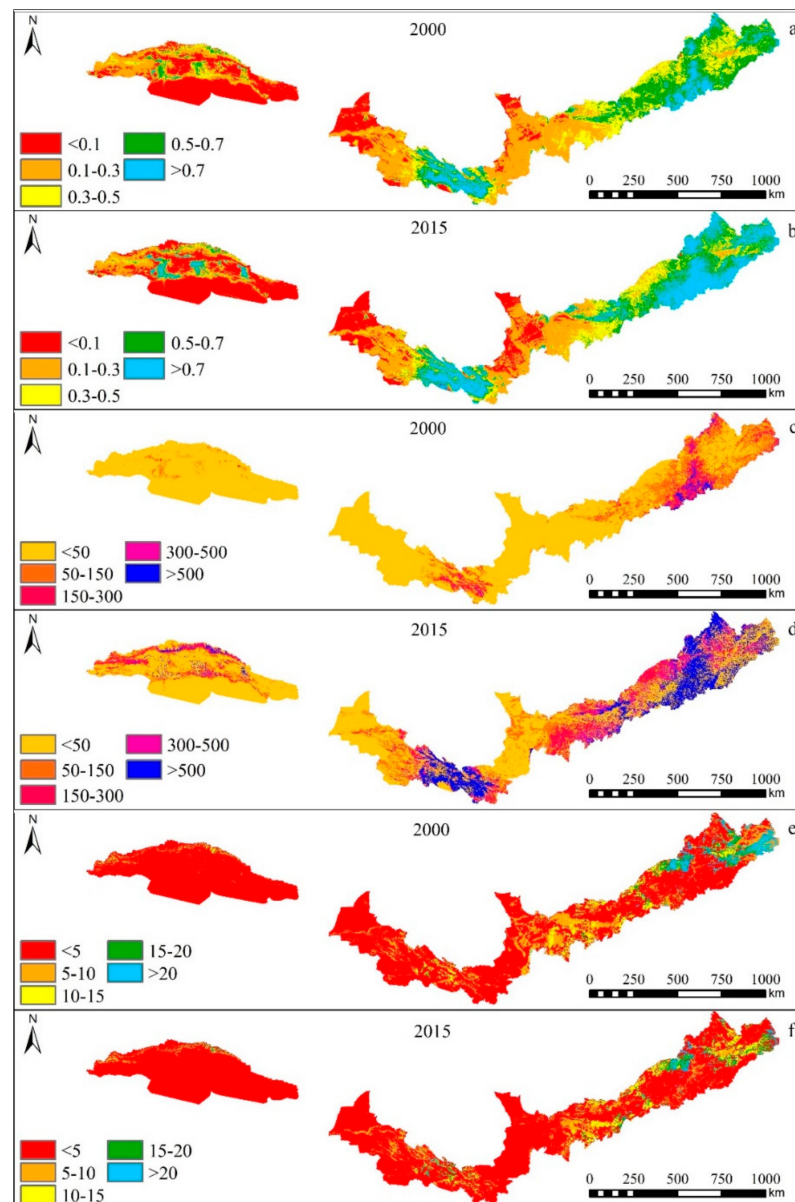

Figure 5. Spatial distribution of vegetation coverage (**a**,**b**), net primary productivity (**c**,**d**), and amount of sand fixation (**e**,**f**) in the northern sand prevention belt of China in 2000 and 2015.

3.2. Spatiotemporal Dynamics of Ecological Vulnerability

The ecological vulnerability index (EVI) displayed the low values in the eastern part of the study region and high values in the western part of the study region in 2000 and 2015 (Figure 6a,b). The EVI ranged from 0.29 to 1.32 in 2000, with the mean value of 0.88, whereas it averaged 0.78 in 2015, ranging from 0.21 to 1.26. In 2000, the area proportion of slightly, lightly, moderately, heavily and extremely vulnerable levels was 2.24%, 8.75%, 13.70%, 26.59% and 48.72% in 2000, respectively, while it was 2.33%, 10.04%, 21.85%, 23.57% and 42.21% in 2015, respectively (Table 3 and Figure 6c,d). During 2000–2015, the proportion area of slightly, lightly, and moderately vulnerable levels increased by 0.09%, 1.29%, and 8.15%, respectively, whereas the area proportion of heavily and extremely vulnerable levels decreased by 3.02% and 6.51%, respectively.
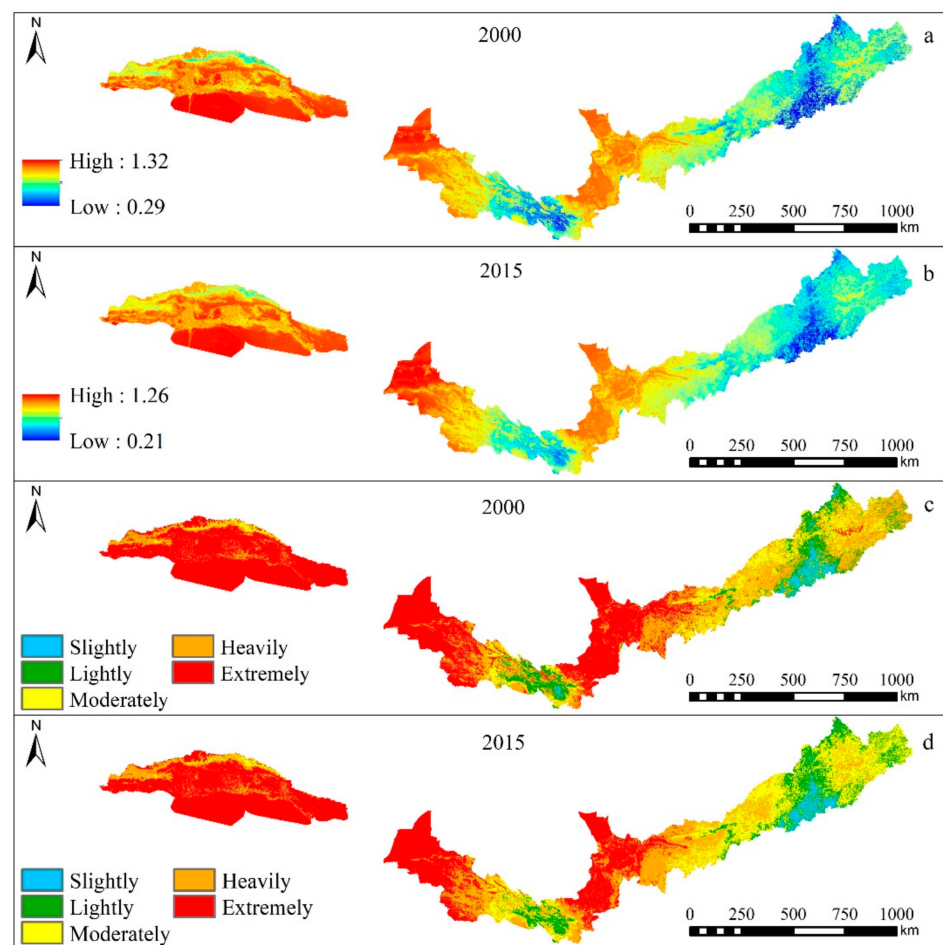

Figure 6. Spatial distribution of ecological vulnerability index (**a**,**b**) and ecological vulnerability levels (**c**,**d**) of northern sand prevention belt of China in 2000 and 2015.

Table 3. The ecological vulnerability levels of the study region in 2000 and 2015.

Year	Area (km^2)	Percentage of Ecological Vulnerability Levels (%)				
		Slightly	Lightly	Moderately	Heavily	Extremely
2000	869,650	2.24	8.75	13.70	26.59	48.72
2015	869,650	2.33	10.04	21.85	23.57	42.21

4. Discussion

Ecological vulnerability assessment has become an important means for recognizing ecological conditions, which can aid sustainable development and ecological restora-

tion [50]. Therefore, numerous studies on ecological vulnerability assessment have been conducted in different landscape types and regions. For example, Ortega et al. [51] assessed the spatial resilience of the Spanish olive socioecological landscape in Spain and found that the index of spatial resilience of olive landscapes was low in southern Spain and medium in the northeast and central Spain, with an increase in it throughout the time series considered. Christmann et al. [52] assessed the vulnerability and resilience constructions in Lübeck and Rostock cities based on the heuristic model for empirical analysis. Anjos and de Toledo [53] assessed the resilience and sensitivity of ecosystems to climate stress of three stable states of ecosystems (forest, savanna, and grassland) in South America. They found that forests are more vulnerable to climate change than savannas or grasslands, and showed less resistance to climate stress. In the present study, the ecological vulnerability of sandy land ecosystems of the NSPB in China was assessed. The ecological vulnerability level of the overall NSPB could be assessed as "extremely" since it occupied the largest area proportions over 42% (Table 3). In addition, the area proportion of "moderately," "heavily," and "extremely" ecological vulnerability levels accounted for more than 87% in both 2000 and 2015 (Figure 6c,d and Table 3). This was consistent with the findings of previous studies. For example, Zou et al. [54] reported that ecological vulnerability is higher in northern China than that in southern China and higher in western China than that in eastern China. Liu et al. [55] demonstrated that the ecological vulnerability of the NSPB was high, compared with other regions of China. In the present study, the high ecological vulnerability of the NSPB was because the study region was located in the arid and semi-arid regions with low annual precipitation (Figure 4a,b), and the vegetation coverage was low (Figure 5a,b). The prosperity of green vegetation is the dominant driving force among all selected indicators due to its ecosystem functions in wind prevention and sand fixation, water and soil conservation, biodiversity, and climate adjustment. Climate factors such as precipitation are basic environmental factors influencing vegetation dynamics. Therefore, low vegetation coverage and low precipitation resulted in high ecological vulnerability (Table 1, Negative). Furthermore, most deserts and sandy land were distributed in the study region., e.g., the Taklimakan Desert, Badain Jaran Desert, Tengger Desert, Hunshan-dak Sand Land, and Horqin Sandy Land [55,56]. Therefore, the ecological vulnerability level of the NSPB overall was high. Moreover, we found that the western part of the study region was suffering from the highest ecological vulnerability (Figure 6a,b). This was because the annual precipitation in this region was less than 100 mm. Additionally, the high altitudes, accompanied by high temperatures, can lead to its bare and sparsely vegetated land cover, which is highly vulnerable to natural and anthropic pressures. Furthermore, deserts and sandy lands were distributed in these regions, with severe desertification and salinization. Therefore, the ecological status of these regions was poor. However, the eastern part of the study region had a low ecological vulnerability index, indicating that this region had a relatively good ecological environment. This was associated with high annual precipitation, vegetation coverage, and net primary productivity (Figures 4 and 5). Although these regions had higher human activity pressure and economic pressure, they had higher resilience. These findings indicated that the ecological vulnerability index was significantly different in different regions. Therefore, we should take differential strategies in different restoration zones, and pay more attention to the improvement of ecological status in the western parts of the study region.

In addition, we observed that the EVI displayed decreasing trend from 2000 to 2015, indicating the ecological status was improved. Similar to our findings, Su et al. [37] reported that the ecological environment of NSPB was improved from 2005 to 2015 based on analyzing the spatial and temporal variations of ecosystem patterns in NSPB. In the present study, decreasing EVI from 2000 to 2015 might be associated with the conduction of environmental protection projects, such as the Three-North Afforestation Program (TNAP, initiated in 1978), Sand Prevention and Control Projects (initiated in 1991), and Grain for Green Program (GGP, initiated in 1999) [57,58]. With the implementation of environmental protection projects, a large number of vegetations had been planted, and

human grazing and farming behaviors had been restricted, which reduced the fragmentation of the landscape and increased vegetation coverage and thus reduced the level of ecological vulnerability. It can be seen that a series of environmental protection measures to improve vegetation coverage are very effective in improving the ecological environment (e.g., increasing sand fixation and reducing soil erosion) [3]. Moreover, with the concept of environmental protection, the economic development of the study region was mostly driven by green industry and ecological engineering, which also contribute to reducing the level of ecological vulnerability. This was demonstrated by the coincident spatial distribution of EVI, vegetation coverage, and net primary productivity (Figures 5 and 6). Moreover, since eco-environmental conservation and construction plans for NSPB were adopted earlier, and the ecological environment of NSPB would promote vegetation growth, great achievements may have been accomplished by eco-environmental projects in the NSPB.

Moreover, we found that the area proportion of "slightly," "lightly," and "moderately" ecological vulnerability levels increased, while the area proportion of "heavily" and "extremely" vulnerability levels decreased, which was associated with the change in the spatial distribution of vegetation coverage, indicating that eco-environmental protection projects were indeed effective in ecological restoration of the NSPB. Therefore, eco-environmental protection projects should be reinforced to improve the ecological restoration of the NSPB.

5. Conclusions

To assess the ecosystem vulnerability of the sand prevention belt in northern China, the ecological pressure–sensibility–resilience model, combined with principal component analysis, was used to assess the ecological vulnerability from 2000 to 2015. The ecological vulnerability index (EVI) displayed low values in the eastern part of the study region and high values in the western part of the study regions. A decrease in EVI from 2000 to 2015 indicated that the ecological status of the study region has been improved due to implement of ecological restoration projects. In addition, the ecological vulnerability level of the overall NSPB could be assessed as "extremely." Furthermore, the area proportion of "slightly," "lightly," and "moderately" ecological vulnerability levels increased from 2000 to 2015, whereas the proportion of "heavily" and "extremely" ecological vulnerability levels decreased, indicating that eco-environmental protection projects were indeed effective in ecological restoration of the NSPB. These findings indicated that differential strategies in different restoration zones should be adopted, especially in the western parts of the study region, and eco-environmental protection projects should be reinforced to improve the ecological restoration of the NSPB. In the western part of the study region with the high ecological vulnerability, some measures such as increasing the vegetation coverage with shrub and grass, and fencing should be adopted to restore the environment, whereas in the eastern part of the study region with relatively low ecological vulnerability, improving quality of vegetation coverage and the adjustment of industrial toward the development of green economy should be encouraged. In addition, the ecological pressure–sensibility–resilience model, combined with principal component analysis, could be applied to assess the ecological vulnerability of other regions due to its comprehensiveness and objectivity. Our findings would supply some scientific references for ecological protection and restoration in ecologically vulnerable regions.

Author Contributions: Conceptualization, L.S.; formal analysis, Z.X. and T.W.; investigation, X.Z., J.L. and L.L.; writing—original draft preparation, X.L. and L.S.; writing—review and editing, L.S. and T.G. All authors have read and agreed to the published version of the manuscript.

Institutional Review Board Statement: Not applicable.

Informed Consent Statement: Not applicable.

Data Availability Statement: Not applicable.

References

1. Zhang, G.L.; Dong, J.W.; Xiao, X.M.; Hu, Z.M.; Sheldon, S. Effectiveness of ecological restoration projects in Horqin Sandy Land, China based on SPOT-VGT NDVI data. *Ecol. Eng.* **2012**, *38*, 20–29. [CrossRef]
2. Staudinger, M.D.; Grimm, N.B.; Staudt, A.; Carter, S.L.; Chapin, F.S. *Impacts of Climate Change on Biodiversity, Ecosystems, and Ecosystem Services: Technical Input to the 2013 National Climate Assessment*; Cooperative Report to the 2013 National Climate Assessment; United States Global Change Research Program: Washington, DC, USA, 2012.
3. Li, Q.; Shi, X.Y.; Wu, Q.Q. Effects of protection and restoration on reducing ecological vulnerability. *Sci. Total Environ.* **2021**, *761*, 143180. [CrossRef]
4. Hu, X.J.; Ma, C.M.; Huang, P.; Guo, X. Ecological vulnerability assessment based on AHP-PSR method and analysis of its single parameter sensitivity and spatial autocorrelation for ecological protection—A case of Weifang City, China. *Ecol. Indic.* **2021**, *125*, 107464. [CrossRef]
5. De Lange, H.J.; Sala, S.; Vighi, M.; Faber, J.H. Ecological vulnerability in risk assessment—A review and perspectives. *Sci. Total Environ.* **2020**, *408*, 3871–3879. [CrossRef] [PubMed]
6. Beroya-Eitner, M.A. Ecological vulnerability indicators. *Ecol. Indic.* **2016**, *60*, 329–334. [CrossRef]
7. Weißhuhn, P.; Müller, F.; Wiggering, H. Ecosystem vulnerability review: Proposal of an interdisciplinary ecosystem assessment approach. *Environ. Manag.* **2018**, *61*, 904–915. [CrossRef] [PubMed]
8. Hou, K.; Tao, W.D.; Wang, L.M.; Li, X.X. Study on hierarchical transformation mechanisms of regional ecological vulnerability and its applicability. *Ecol. Indic.* **2020**, *114*, 106343. [CrossRef]
9. Zimmerman, J.K.; Willig, M.R.; Hernández-Delgado, E.A. Resistance, resilience, and vulnerability of social-ecological systems to hurricanes in Puerto Rico. *Ecosphere* **2020**, *11*, e03159. [CrossRef]
10. Hong, W.Y.; Jiang, R.R.; Yang, C.Y.; Zhang, F.F.; Su, M.; Liao, Q. Establishing an ecological vulnerability assessment indicator system for spatial recognition and management of ecologically vulnerable areas in highly urbanized regions: A case study of Shenzhen, China. *Ecol. Indic.* **2016**, *69*, 540–547. [CrossRef]
11. Xia, M.; Jia, K.; Zhao, W.W.; Liu, S.L.; Wei, X.Q.; Wang, B. Spatio-temporal changes of ecological vulnerability across the Qinghai-Tibetan Plateau. *Ecol. Indic.* **2021**, *123*, 107274. [CrossRef]
12. Ghiasvand, F.; Babaei, A.A.; Yazdani, M.; Birgani, Y.T. Spatial modeling of environmental vulnerability in the biggest river in Iran using geographical information systems. *J. Environ. Health Sci. Eng.* **2021**. [CrossRef]
13. Song, G.B.; Li, Z.; Yang, Y.G.; Semakula, H.M.; Zhang, S.S. Assessment of ecological vulnerability and decision-making application for prioritizing roadside ecological restoration: A method combining geographic information system, Delphi survey and Monte Carlo simulation. *Ecol. Indic.* **2015**, *52*, 57–65. [CrossRef]
14. Dzoga, M.; Simatele, D.; Munga, C. Assessment of ecological vulnerability to climate variability on coastal fishing communities, A study of Ungwana Bay and Lower Tana Estuary, Kenya. *Ocean Coast. Manag.* **2018**, *163*, 437–444. [CrossRef]
15. Xie, Z.L.; Li, X.Z.; Jiang, D.G.; Li, S.W.; Yang, B.; Chen, S.L. Threshold of island anthropogenic disturbance based on ecological vulnerability Assessment-A case study of Zhujiajian Island. *Ocean Coast. Manag.* **2019**, *167*, 127–136. [CrossRef]
16. Shi, H.H.; Lu, J.F.; Zheng, W.; Sun, J.K.; Li, J.; Guo, Z.; Huang, J.T.; Yu, S.T.; Yin, L.T.; Wang, Y.Z.; et al. Evaluation system of coastal wetland ecological vulnerability under the synergetic influence of land and sea: A case study in the Yellow River Delta, China. *Mar. Pollut. Bull.* **2020**, *161*, 111735. [CrossRef] [PubMed]
17. Xue, L.Q.; Wang, J.; Zhang, L.C.; Wei, G.H.; Zhu, B.L. Spatiotemporal analysis of ecological vulnerability and management in the Tarim River Basin, China. *Sci. Total Environ.* **2019**, *649*, 876–888. [CrossRef] [PubMed]
18. Berrouet, L.M.; Machado, J.; Villegas-Palacio, C. Vulnerability of socio-ecological systems, A conceptual framework. *Ecol. Indic.* **2018**, *84*, 632–647. [CrossRef]
19. Zhou, J.H.; Huang, X.X. A review on the assessment methods of ecological vulnerability. *Yunnan Geogr. Environ. Res.* **2008**, *20*, 55–60.
20. Zhong, X.J.; Sun, B.P.; Zhao, Y.; Li, J.R.; Zhou, X.S.; Wang, Y.Q.; Qiu, Y.D.; Feng, L. Ecological vulnerability evaluation based on principal component analysis in Yunnan province. *Ecol. Environ. Sci.* **2011**, *20*, 109–113.
21. Yu, X.; Li, Y.; Xi, M.; Kong, F.L.; Pang, M.Y.; Yu, Z.D. Ecological vulnerability analysis of Beidagang National Park, China. *Front. Earth Sci.* **2019**, *13*, 385–397. [CrossRef]
22. Li, R.; Han, R.; Yu, Q.R.; Qi, S.; Guo, L. Spatial heterogeneous of ecological vulnerability in arid and semi-arid area: A case of the Ningxia Hui Autonomous Region, China. *Sustainability* **2020**, *12*, 4401. [CrossRef]
23. Ghosh, S.; Das, A. Urban expansion induced vulnerability assessment of East Kolkata Wetland using Fuzzy MCDM method. *Remote Sens. Lett.* **2019**, *13*, 191–203. [CrossRef]
24. Li, L.W.; Liu, Z.; Bai, Y.L.; Sheng, J. Environmental vulnerability evaluation of Yellow River Delta coast based on AHP-CVI technology. *Ecol. Environ. Sci.* **2018**, *27*, 297–303.

25. Wu, C.S.; Liu, G.H.; Huang, C.; Liu, Q.S.; Guan, X.D. Ecological vulnerability assessment based on fuzzy analytical method and analytic hierarchy process in Yellow River Delta. *Int. J. Environ. Res. Pub. Health* **2018**, *15*, 855. [CrossRef]

26. Park, Y.S.; Chon, T.S.; Kwak, I.S.; Lek, S. Hierarchical community classification and assessment of aquatic ecosystems using artificial neural networks. *Sci. Total Environ.* **2004**, *327*, 105–122. [CrossRef]

27. Guo, B.; Kong, W.H.; Han, F.; Wang, J.J.; Jiang, L.; Lu, Y.F. Dynamic monitoring of ecological vulnerability in the semi-arid desert and steppe ecological zone of Northern China based on RS and its driving mechanism analysis. *J. Tropical Subtropical Bot.* **2018**, *26*, 1–12, (In Chinese with English abstract).

28. Defne, Z.; Aretxabaleta, A.L.; Ganju, N.K.; Kalra, T.S.; Jones, D.K.; Smith, K.E.L. A geospatially resolved wetland vulnerability index: Synthesis of physical drivers. *PLoS ONE* **2020**, *15*, e0228504. [CrossRef]

29. Malekmohammadi, B.; Jahanishakib, F. Vulnerability assessment of wetland landscape ecosystem services using driver-pressure-state-impact-response (DPSIR) model. *Ecol. Indic.* **2017**, *82*, 293–303. [CrossRef]

30. Ippolito, A.; Sala, S.; Faber, J.H.; Vighi, M. Ecological vulnerability analysis: A river basin case study. *Sci. Total Environ.* **2010**, *408*, 3880–3890. [CrossRef] [PubMed]

31. Pang, L.H.; Kong, F.L.; Xi, M.; Li, Y. Spatio-temporal changes of ecological vulnerability in the Jiaozhou Bay coastal zone. *J. East China Normal Univ.* **2018**, *3*, 222–233.

32. Bueno-Pardo, J.; Nobre, D.; Monteiro, J.N.; Sousa, P.M.; Costa, E.F.S.; Baptista, V.; Ovelheiro, A.; Vieira, V.M.N.C.S.; Chícharo, L. Climate change vulnerability assessment of the main marine commercial fish and invertebrates of Portugal. *Sci. Rep.* **2021**, *11*, 2958. [CrossRef] [PubMed]

33. Nguyen, A.K.; Liou, Y.A.; Li, M.H.; Tran, T.A. Zoning eco-environmental vulnerability for environmental management and protection. *Ecol. Indic.* **2016**, *69*, 100–117. [CrossRef]

34. Yang, H.F.; Zhai, G.F.; Zhang, Y. Ecological vulnerability assessment and spatial pattern optimization of resource-based cities: A case study of Huaibei City, China. *Hum. Ecol. Risk Assess.* **2021**, *27*, 606–625. [CrossRef]

35. Zolkos, S.G.; Jantz, P.; Cormier, T.; Iverson, L.R.; McKenney, D.W.; Goetz, S.J. Projected tree species redistribution under climate change: Implications for ecosystem vulnerability across protected areas in the Eastern United States. *Ecosystems* **2015**, *18*, 202–220. [CrossRef]

36. Wang, X.F.; Li, Y.H.; Chu, B.Y.; Liu, S.R.; Yang, D.; Luan, J.W. Spatiotemporal dynamics and driving forces of ecosystem changes: A case study of the national barrier zone, China. *Sustainability* **2020**, *12*, 6680. [CrossRef]

37. Su, K.; Sun, X.T.; Wang, Y.R.; Chen, L.; Yue, D.P. Spatial and temporal variations of ecosystem patterns in Northern sand control barrier belt based on GIS and RS. *Trans. Chin. Soc. Agric. Mach.* **2020**, *51*, 226–236, (In Chinese with English abstract).

38. Aronson, J.; Goodwin, N.; Orlando, L.; Eisenberg, C.; Cross, A.T. A world of possibilities: Six restoration strategies to support the United Nation's Decade on Ecosystem Restoration. *Restor. Ecol.* **2020**, *28*, 730–736. [CrossRef]

39. Zhang, X.Q.; Wang, L.K.; Fu, X.S.; Li, H.; Xu, C.D. Ecological vulnerability assessment based on PSSR in Yellow River Delta. *J. Clean. Prod.* **2017**, *167*, 1106–1111. [CrossRef]

40. Wei, W.J.; Wang, B.; Niu, X. Soil erosion reduction by Grain for Green Project in desertification areas of Northern China. *Forests* **2020**, *11*, 473. [CrossRef]

41. Chen, X.W.; Li, X.M.; Eladawy, A.; Yu, T.; Sha, J.M. A multi-dimensional vulnerability assessment of Pingtan Island (China) and Nile Delta (Egypt) using ecological Sensitivity-Resilience-Pressure (SRP) model. *Hum. Ecol. Risk Assess.* **2021**. [CrossRef]

42. Hou, K.; Li, X.X.; Zhang, J. GIS analysis of changes in ecological vulnerability using a SPCA Model in the Loess Plateau of Northern Shaanxi, China. *Int. J. Environ. Res. Public Health* **2015**, *12*, 4292–4305. [CrossRef]

43. Yang, Y.J.; Ren, X.F.; Zhang, S.L.; Chen, F.; Hou, H.P. Incorporating ecological vulnerability assessment into rehabilitation planning for a post-mining area. *Environ. Earth Sci.* **2017**, *76*, 245. [CrossRef]

44. Lv, X.J.; Xiao, W.; Zhao, Y.L.; Zhang, W.K.; Li, S.C.; Sun, H.X. Drivers of spatio-temporal ecological vulnerability in an arid, coal mining region in Western China. *Ecol. Indic.* **2019**, *106*, 105475. [CrossRef]

45. Zou, T.H.; Yoshino, K. Environmental vulnerability evaluation using a spatial principal component approach in the Daxing'anling region, China. *Ecol Indic.* **2017**, *78*, 405–415. [CrossRef]

46. Sun, P.J.; Xiu, C.L.; Wang, Z.Z. Assessment of Ming-city's ecological-fragility on changes based on the PSE model. *Econ. Geogr.* **2010**, *30*, 1354–1359, (In Chinese with English abstract).

47. Kerner, D.A.; Thomas, J.S. Resilience attributes of social-ecological systems: Framing metrics for management. *Resources* **2014**, *3*, 672–702. [CrossRef]

48. Jarraha, M.; Mayel, S.; Tatarko, J.; Funk, R.; Kuka, K. A review of wind erosion models: Data requirements, processes, and validity. *Catena* **2020**, *187*, 104388. [CrossRef]

49. Dossou, J.F.; Li, X.X.; Sadek, M.; Almouctar, M.A.S.; Mostafa, E. Hybrid model for ecological vulnerability assessment in Benin. *Sci. Rep.* **2021**, *11*, 2449. [CrossRef] [PubMed]

50. Guo, B.; Fan, Y.W.; Yang, F.; Jiang, L.; Yang, W.N.; Chen, S.T.; Gong, R.; Liang, T. Quantitative assessment model of ecological vulnerability of the Silk Road Economic Belt, China, utilizing remote sensing based on the partition–integration concept. *Geomat. Nat. Hazards Risk* **2019**, *10*, 1346–1366. [CrossRef]

51. Ortega, M.; Pascual, S.; Elena-Rosselló, R.; Rescia, A.J. Land-use and spatial resilience changes in the Spanish olive socio-ecological landscape. *Appl. Geogr.* **2020**, *117*, 102171. [CrossRef]

52. Christmann, G.B.; Balgar, K.; Mahlkow, N. Local constructions of vulnerability and resilience in the context of climate change. A comparison of Lübeck and Rostock. *Soc. Sci.* **2014**, *3*, 142–159. [CrossRef]

53. Anjos, L.J.; de Toledo, P.M. Measuring resilience and assessing vulnerability of terrestrial ecosystems to climate change in South America. *PLoS ONE* **2018**, *13*, e0194654. [CrossRef] [PubMed]

54. Zou, H.; Duan, X.J.; Ye, L.; Wang, L. Locating sustainability issues: Identification of ecological vulnerability in Mainland China's Mega-Regions. *Sustainability* **2017**, *9*, 1179. [CrossRef]

55. Liu, J.H.; Zou, C.X.; Gao, J.X.; Ma, S.; Wang, W.J.; Wu, K.; Liu, Y. Location determination of ecologically vulnerable regions in China. *Bio. Sci.* **2015**, *23*, 725–732. [CrossRef]

56. Zhu, F.Y.; Lu, H.Y.; Zhang, W.C.; Chen, Y.Y.; Zeng, L.; Xu, Z.W.; Zhang, H.Z.; Dong, L.N. Mapping deserts and sandy fields in Northern China and surface process analysis based on 3S techniques. *Quat. Sci.* **2013**, *33*, 197–205, (In Chinese with English abstract).

57. Zhu, J.J.; Zheng, X.; Yan, Q.L. *Assessment of Impacts of the Three-North Protective Forest Program on Ecological Environments by Remote Sensing Technology-Launched after 30 Years (1978–2008)*; Science Press: Beijing, China, 2016.

58. Zhu, J.J.; Song, L.N. A review of ecological mechanisms for management practices of protective forests. *J. For. Res.* **2021**, *32*, 435–448. [CrossRef]